ON THE ELECTROMECHANICAL BEHAVIOUR OF THIN PERFORATED BACKPLATES IN SILICON CONDENSER MICROPHONES

M. Pedersen, W. Olthuis and P. Bergveld

MESA Research Institute, University of Twente, P.O. Box 217, NL-7500 AE Enschede, The Netherlands

SUMMARY

In this work an alternative approach to the modelling of plates with a large number of holes, is presented. By means of plate theory, it is shown that perforated plates can be modelled by conventional orthotropic plates with modified elastic properties. The modification of the elastic constants is derived by equalising the strain-energy of the perforated and the orthotropic plate. The model obtained is then compared with previous methods and applied in the electromechanical simulation of a silicon micromachined microphone structure. The microphone structures are simulated numerically, using an algorithm based on finite differences.

INTRODUCTION

In the development of sensors, the silicon micromachining technology has proven to be very useful. Mechanical devices with dimensions, which were impossible to manufacture with conventional technologies, are now feasible. Furthermore, by introducing the new technology it is sometimes possible to enhance the functionality and the performance of the sensors. A good example of this is the development of the silicon condenser microphone (figure 1). The condenser microphone basically consists of a parallel plate capacitor, where one plate is sensitive to the sound pressure.

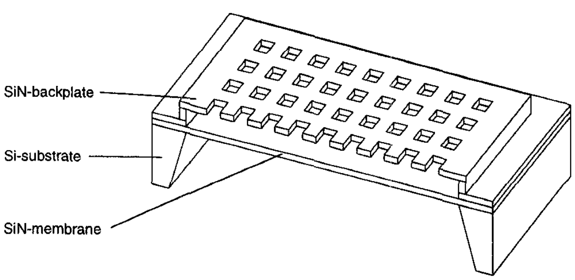

Figure 1: A silicon condenser microphone [1].

The static bias voltage required over the plates is 50-200 V for conventional microphones, which is normally achieved by using an electret in the air gap of the microphone. By the introduction of silicon micromachining, it has become possible to reduce the air gap between the two plates from >30 μm to 1-3 μm [1,2], thereby reducing the required bias voltage to 5-15 V, which can be applied externally with a small battery and a voltage multiplier. The electret can therefore be omitted, and the long term drift problems normally associated with these devices can be avoided.

The downscaling, however, also means that control of the airflow in the gap, which directly influences the upper cut-off frequency of the microphone, becomes a critical design criterion. In order to sufficiently reduce the flow resistance in the gap, a large amount of holes is required in the backplate. If the thickness of the backplate is comparable with the thickness of the membrane, a reduction of the rigidity, due to the holes, may have a significant influence on the behaviour of the microphone. In the field of microsensors this problem has not yet been considered in detail, mainly due to limited use of perforated membranes. For silicon condenser microphones, it has until now been common to use the simple assumption, that the elastic properties of the perforated plate could be described by a solid plate with a thickness reduced by the same fraction as the surface area occupied by the holes [3].

In this paper, an alternative, more complex, model of the perforated plate is presented, and the differences with the simple model are investigated, both for single plates and for plates in a microphone structure. Since the theory is of general nature, it can be useful in any application containing a perforated plate.

DEFLECTION OF PERFORATED PLATES

Calculating the mechanical parameters of a perforated plate proves to be difficult. It is well known that stress concentrations appear around holes in deflected plates, however, the only accurate way to obtain this stress distribution is to insert the boundary conditions of a free edge on the edges of each hole [4]. This is already a complex task for a square plate with one hole, and if the plate contains several thousand holes, this method must in reality be considered impossible.

A different approach is to model the perforated plate by a solid plate with pseudo elastic constants and mass. This theory has previously been applied for large scale mechanical constructions [5,6]. The idea is to equal the strain-energy of a small element in a solid plate with the energy of a similar element in a perforated plate. For simplicity it is assumed that the holes in the perforated plate are squares, and that they are placed in a regular pattern (figure 2).

From the definition of the stress-strain relations in an orthotropic plate, the bending moments are given by [4]:

$$M_x = -\frac{h^3}{12}\left(C_{11}\frac{\partial^2 w}{\partial x^2}+C_{12}\frac{\partial^2 w}{\partial y^2}\right)$$
$$M_y = -\frac{h^3}{12}\left(C_{21}\frac{\partial^2 w}{\partial x^2}+C_{22}\frac{\partial^2 w}{\partial y^2}\right) \quad (1)$$
$$M_{xy} = \frac{h^3}{6}C_{44}\frac{\partial^2 w}{\partial x \partial y}$$

where h is the plate thickness, $C_{11}=C_{22}$, $C_{12}=C_{21}$ and C_{44} are material constants, $w(x,y)$ is the deflection function, and x, y are the primary directions of the plane of the plate. The strain energy dV_{bs} from bending of a small element $dxdy$ of the plate is then [4]:

$$dV_{bs} =$$
$$-\frac{1}{2}\left[M_x\frac{\partial^2 w}{\partial x^2}+M_y\frac{\partial^2 w}{\partial y^2}-\left(M_{xy}\frac{\partial^2 w}{\partial x\partial y}+M_{yx}\frac{\partial^2 w}{\partial y\partial x}\right)\right]dxdy=$$
$$\frac{h^3}{24}\left[C_{11}\left(\frac{\partial^2 w}{\partial x^2}\right)^2+C_{22}\left(\frac{\partial^2 w}{\partial y^2}\right)^2+2C_{12}\frac{\partial^2 w}{\partial x^2}\frac{\partial^2 w}{\partial y^2}+4C_{44}\left(\frac{\partial^2 w}{\partial y\partial x}\right)^2\right]dxdy \quad (2)$$

In addition to this, the contribution from eventual built-in stress should be included. This energy dV_{ss} can be expressed by the following equation [4]:

$$dV_{ss} = \frac{1}{2}\left(N_x\varepsilon_x + N_y\varepsilon_y\right)dxdy \quad (3)$$

where N_x, N_y, ε_x and ε_y are built-in forces and strains in the middle plane of the plate. By use of the force-strain relations [4] and $N_x = N_y = \sigma \cdot h$, the equation can be rewritten to:

$$dV_{ss} = \frac{1}{2hE}\left[N_x\left(N_x - \nu N_y\right)+N_y\left(N_y-\nu N_x\right)\right]dxdy$$
$$= \frac{h(1-\nu)\sigma^2}{E}dxdy \quad (4)$$

where E is Young's modulus, ν is Poisson's ratio and σ is the built-in stress. It should be noted that this energy only depends on the built-in stress, since it is assumed that no strains are induced in the middle plane by the deflection.

The total strain-energy of a bent element in a solid orthotropic plate is then:

$$dV_{ts} = dV_{bs} + dV_{ss} =$$
$$\frac{h^3}{24}\left[C_{11}\left(\frac{\partial^2 w}{\partial x^2}\right)^2+C_{22}\left(\frac{\partial^2 w}{\partial y^2}\right)^2+2C_{12}\frac{\partial^2 w}{\partial x^2}\frac{\partial^2 w}{\partial y^2}+4C_{44}\left(\frac{\partial^2 w}{\partial y\partial x}\right)^2\right]dxdy$$
$$+\frac{h(1-\nu)\sigma^2}{E}dxdy \quad (5)$$

Considering the basic element in the perforated plate (figure 2), it can be seen that the element may be regarded as one small plate, with sidelength b-$2a$, and four beam tips with length a. By calculating the strain-energy of these parts [6], it can be shown that the strain-energy dV_{bp} from bending of the basic element with sidelength b is:

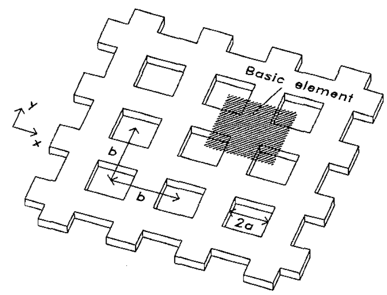

Figure 2: Perforated plate with square holes in a regular pattern.

$$V_{bp} =$$
$$\frac{Eh^3}{24}\left[\left\{\frac{b(b-2a)}{1-\nu^2}+\frac{a(b-2a)^2}{b}\right\}\left\{\left(\frac{\partial^2 w}{\partial x^2}\right)^2+\left(\frac{\partial^2 w}{\partial y^2}\right)^2\right\}\right.$$
$$+\frac{2\nu b(b-2a)}{1-\nu^2}\frac{\partial^2 w}{\partial x^2}\frac{\partial^2 w}{\partial y^2}$$
$$\left.+\frac{1}{1+\nu}\left\{2b(b-2a)+\frac{12Ka(b-2a)}{bh^3}\right\}\left(\frac{\partial^2 w}{\partial x\partial y}\right)^2\right] \quad (6)$$

where K is a constant defined by:

$$K = \begin{cases} \frac{1}{3}\left(1-0.63\frac{b-2a}{h}\right)(b-2a)^3 h & \text{for } h > b-2a \\ \frac{1}{3}\left(1-0.63\frac{h}{b-2a}\right)(b-2a)h^3 & \text{for } h < b-2a \end{cases} \quad (7)$$

As mentioned above, the strain-energy induced by the built-in stress dV_{sp} is considered to be independent of the plate deflection. Therefore, it may be assumed that the expression (4) can be used, by simply reducing it by the same factor with which the element area is reduced by the holes.

$$dV_{sp} = \left(1-\frac{4a^2}{b^2}\right)\frac{h(1-\nu)\sigma^2}{E}dxdy \quad (8)$$

The total strain-energy for the bent element in figure 2 is therefore:

$$V_{tp} = V_{bp} + \frac{4h\left(b^2-4a^2\right)(1-\nu)\sigma^2}{E} \quad (9)$$

By equalising this expression with the expression (5) for an orthotropic solid element with sidelength b, the pseudo material constants of the perforated plate can be derived:

$$C_{11} = C_{22} = \frac{E}{b^2}\left\{\frac{b(b-2a)}{1-\nu^2}+\frac{a(b-2a)^2}{b}\right\} \quad (10)$$

$$C_{12} = C_{21} = \frac{\nu E(b-2a)}{b\left(1-\nu^2\right)} \quad (11)$$

$$C_{44} = \frac{E}{4b^2(1+\nu)}\left\{2b(b-2a)+\frac{12Ka(b-2a)}{bh^3}\right\} \quad (12)$$

It is now possible to use these modified elastic constants in a normal calculation, meaning that a solid plate is assumed to have the elastic properties of a perforated plate. The same thing can be done with the built-in stress. It may be seen from (8) that the strain-energy from stress has been reduced by a factor ($1-4a^2/b^2$). This can be translated into a solid plate having a built-in stress of $\sqrt{1-4a^2/b^2}\cdot\sigma$.

PLATE ANALYSIS

The deflection of a plate with built-in stress, subjected to an external lateral load $q(x,y)$, is described by the following differential equation [4]:

$$\frac{\partial^2 M_x}{\partial x^2} - 2\frac{\partial^2 M_{xy}}{\partial x \partial y} + \frac{\partial^2 M_y}{\partial y^2} + \sigma h \nabla^2 w = -q \quad (13)$$

By substitution of eqs. (1) and (10)-(12) in (13), a fourth degree differential equation of the deflection $w(x,y)$ is obtained. An analytical solution to this equation with the boundary conditions of built-in edges, is not known.

A numerical method suited for solving this equation is finite differences, which has previously been applied for orthotropic plates [7]. By discretisation of the function $w(x,y)$ in an n×n grid, the discrete version of (13) can be used to write a linear equation for each point on the grid, thereby producing an nth order linear equation system of the form:

$$[A]\cdot[w]=[q] \quad (14)$$

By solving this system, the deflection function for any arbitrary load function $q(x,y)$ can be found.

If the resonance frequency of the plate is to be determined, an additional load from the mass of inertia must be added, yielding:

$$\Psi w + \mu\frac{\partial^2 w}{\partial t^2} = -q(x,y,t) \quad (15)$$

where Ψ is an operator for the actions on $w(x,y,t)$ on the left side of (13), and μ is the surface density of the plate. When analysing a perforated plate, the surface density must be reduced with the hole fraction.

The equation (15) can be solved using the iterative implicit method [8], with a discrete equation of the form:

$$\left([A]+\frac{\mu}{\Delta_t^2}\right)\cdot[w]_{t+1} = -[q]_t + \frac{\mu}{\Delta_t^2}\left(2[w]_t - [w]_{t-1}\right) \quad (16)$$

where Δ_t is discretisation constant in the time domain.

QUASISTATIC MICROPHONE ANALYSIS

The quasistatic deflection of the two thin plates in the condenser microphone structure in figure 1 is given by:

$$D_m \cdot \nabla^4 w_m - \sigma_m h_m \cdot \nabla^2 w_m = p_{ac} + p_{el} \quad (17a)$$

$$\Psi w_b = -\left(1-4a^2/b^2\right)p_{el} \quad (17b)$$

where D_m, σ_m, h_m and $w_m(x,y)$ are the rigidity, built-in stress, thickness and deflection function of the membrane, p_{ac} is the acoustical sound pressure, $w_b(x,y)$ is the deflection function of the backplate, and $p_{el}(x,y)$ is the electrostatic load from the bias voltage V_b across the plates given by:

$$p_{el} = \frac{\varepsilon_0}{2\left(d-w_m-w_b\right)^2}V_b^2 \quad (17c)$$

with ε_0 and d being the permeability and thickness of the air gap between the two plates.

By solving the two non-linear coupled differential equations defined by (17a-c), it is possible to gain important information about quasistatic microphone parameters, like critical bias voltage and maximum allowable sound pressure.

A numerical solution of this complex problem can be obtained by using an iterative finite difference method, where (17a) is first solved with the initial condition $w_b(x,y)=0$. The solution for $w_m(x,y)$ is then used in (17b) to find the new $w_b(x,y)$. This iteration is repeated until the specified relative precision is acquired. Since the function $p_{el}(x,y)$ is monotonously increasing, for increasing $w_m(x,y)$ and $w_b(x,y)$, and since only one solution to (17a+b) exists for the given boundary conditions, it can be proved that the iteration will only converge towards one value.

However, if the bias voltage V_b is too high, the system becomes unstable, and no solution exists. This can be interpreted as a collapse of the structure, and the maximum possible voltage where this can be avoided is named the critical bias voltage. A similar value exists for the quasistatic sound pressure p_{ac}.

RESULTS

The numerical methods described above were implemented with a C-program on an HP-9000 computer system. Due to the assumed symmetry, only one quarter of the plates was simulated.

Simulations of perforated plates with built-in edges have been carried out in order to investigate the influence of the holes. In figures 3 and 4 the first resonance frequency and mechanical sensitivity (center deflection divided by the load) for two different materials (stress-free silicon (Si) and silicon nitride (SiN) with tensile stress (50 MPa)), are shown. Since the results were normalised to a plate having no holes, the specific material parameters are not important. Also shown in the figures is the reduced thickness model (RT-model) of Bergqvist [3]. It may be seen that no close correlation exists between the simple RT-model and the more elaborate strain-energy equalisation (SE-model). In fact, the SiN plate with tensile stress shows an increase of the resonance frequency, as opposed to the decrease predicted by the RT-model. This can be explained by the fact that the mass of the plate decreases faster than the rigidity, thus causing a higher resonance frequency. This is not the case for the stress-free silicon plate, however, the non-linear nature of the SE-model becomes evident at higher hole fractions.

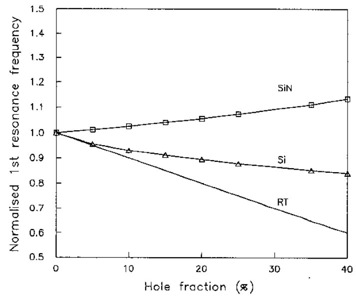

Figure 3: Normalised first resonance frequency for two perforated plates.

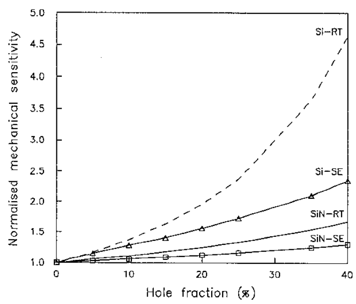

Figure 4: Normalised mechanical sensitivity for two perforated plates.

In figure 4, the normalised mechanical sensitivity calculated with the two models (SE and RT) is shown. It may be seen that a significant difference exists both for the Si plate (Si-SE, Si-RT) and the SiN plate (SiN-SE, SiN-RT), however, the relative difference is smaller for stressed plates.

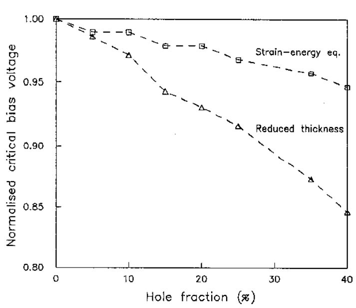

Figure 5: Normalised critical bias voltage for a microphone with the SE- and RT backplate model.

Finally, the relation between the holes in a microphone backplate and two microphone key parameters, the critical bias voltage and the maximum allowable sound pressure (MASP) was investigated. The parameters were calculated using both backplate models (SE, RT) with an SiN membrane and backplate. From the data (figures 5 and 6) it can be seen that a much larger influence of the holes is predicted by the RT-model, than with the SE-model. This tendency coincides well with the previous calculations of the mechanical sensitivity of the backplates (figure 4).

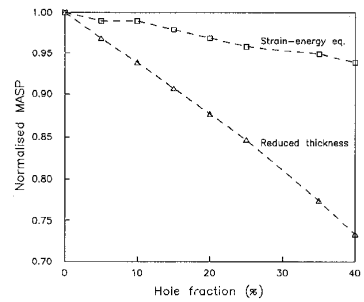

Figure 6: Normalised maximum allowable sound pressure for a microphone with the SE- and RT backplate model.

CONCLUSIONS

In this paper an alternative theory, previously developed for larger plates, has been adopted for the analysis of perforated plates in micromechanical sensors. The model was compared with a simple reduced thickness model. From the investigations it can be concluded that the reduced thickness model may be used as a worst case scenario, however, it does not adequately describe the conditions in the perforated plate. If the strain-energy equalisation is used, it is possible to further optimise the performance of the device containing the perforated plate. The suggested differences between the two models are to be verified experimentally.

ACKNOWLEDGEMENTS

This work is sponsored by the Dutch Research Council.

REFERENCES

[1] Scheeper, P.R; van der Donk, A.G.H; Olthuis, W and Bergveld P, IEEE J. MEMS **1** (1992) 147-154.

[2] Bergqvist, J and Rudolf F, Sens. Actuators A **45** (1994) 115-124.

[3] Bergqvist, J, Sens. Actuators A **39** (1993) 191-200.

[4] Timoshenko S.P and Woinowsky-Krieger S, Theory of plates and shells, McGraw-Hill (1959), New York.

[5] Horvay, G, J. Appl. Mech **19** (1952) 122

[6] Mahoney J.B; Salerno V.L and Goldberg M.A, Bulletin Series / Welding Research Council **82** (1962) New York.

[7] Lee K.W and Wise K.D, IEEE Trans. Electron. Dev **ED-29** (1982) 34-41.

[8] Carnahan, B; Luther, H.A and Wilkes, J.O, Applied Numerical Methods, Wiley (1969), New York.